metals

MDPI

Article

First-Principles Study on the Effect of H, C, and N at the Interface on Austenite/Ferrite Homojunction

Xinghua Zhu [1], Bowen Chen [1], Qingguo Feng [1], Lei Xiao [2], Xiaoyang Zhu [2], Zhiyong Huang [2], Jianguo He [3] and Yi Xu [1,*]

[1] Key Laboratory of Advanced Technologies of Materials, Ministry of Education, School of Materials Science and Engineering, Southwest Jiaotong University, Chengdu 610031, China
[2] Sichuan Liuhe Special Metal Materials Co., Ltd., Mianyang 621700, China
[3] Central Iron & Steel Research Institute, Beijing 100081, China
* Correspondence: xybwbj@swjtu.cn

Abstract: The homojunction provides an effective way to extend the properties of stainless steel, but also leaves more weak points for small atoms to penetrate. In this study, the effects of hydrogen, carbon, and nitrogen atoms at the interface on the austenite/ferrite homojunction were investigated using first principles. This study found that low concentrations of carbon/nitrogen are favorable for the pairing of FCC with BCC compared to hydrogen, which can effectively improve the bonding energy and stability of homogeneous junctions. However, at high concentrations, the interfacial hydrogen can partially act as a mediator for interfacial bonding, which results in a slower decrease in bonding energy. On the contrary, nitrogen causes a sharp decrease in interfacial matching due to excessive strengthening of austenite, which reduces both the binding energy and the stability of the overall system. This study provides valid data and a unique perspective on the development of the austenite/ferrite homojunction.

Keywords: austenite; ferrite; homojunction; density functional theory

check for updates

Citation: Zhu, X.; Chen, B.; Feng, Q.; Xiao, L.; Zhu, X.; Huang, Z.; He, J.; Xu, Y. First-Principles Study on the Effect of H, C, and N at the Interface on Austenite/Ferrite Homojunction. *Metals* **2023**, *13*, 317. https://doi.org/10.3390/met13020317

Academic Editors: Guy Makov and Alain Pasturel

Received: 6 January 2023
Revised: 27 January 2023
Accepted: 1 February 2023
Published: 3 February 2023

Copyright: © 2023 by the authors. Licensee MDPI, Basel, Switzerland. This article is an open access article distributed under the terms and conditions of the Creative Commons Attribution (CC BY) license (https://creativecommons.org/licenses/by/4.0/).

1. Introduction

Stainless steel is a very important alloy with a wide range of applications. It can be found in almost everything from everyday electrical appliances to very complex applications such as structural materials for nuclear reactors [1].

This alloy is based on the iron–chromium system. Meanwhile, many other alloying elements, such as nitrogen, have been introduced in order to obtain specific properties. The microstructure in stainless steel can be divided into three categories based on the composition and content of elements, namely ferrite, austenite, and martensite. These structures can be converted to each other by adjusting the chemical composition [2], which is also known as a phase change. According to these three main microstructures, stainless steel can be further divided into several categories, such as austenitic stainless steel and duplex stainless steel [3,4]. Different properties give them different applications. For instance, a total content of nickel and chromium not less than 23% will help stainless steel to achieve shock-resistant properties [5]. At the same time, it will also bring good high-temperature strength and scaling resistance to stainless steel. Another example is that austenitic stainless steel generally has better corrosion resistance than ferritic and martensitic stainless steel. This is because the single-phase state can stably exist in the austenitic stainless steel, while the carbide segregation phase is easier to form in the martensite and ferrite due to the content of Cr and C [6,7].

However, multi-phase coordination is needed because the performance of single-phase is usually extreme. For example, pure single-phase stainless steel conforms well to the strength–ductility trade-off, which means that their disadvantages are also very prominent (either hard and brittle, or good ductility but low strength). In many cases, the collaboration

of multiple microstructures is required to achieve balanced performance. This strategy has been widely used and derived in many forms such as second-phase reinforcement. However, one of the disadvantages of this strategy is that it allows for the formation of the interface, which is a weak spot compared to other areas. For example, the structure and lattice constants of the second phase are often different from those of the matrix, and the significant strengthening effect is usually caused by the interaction between the dislocation and the elastic strain energy generated by the second phase. These factors comprehensively lead to the potential initiation of cracks near the interface [8,9]. Similarly, lattice distortions at the interface provide opportunities for the penetration of small atoms [10], which may lead to serious degradation of interface performance or even fracture [11,12]. This has been confirmed by a large amount of literature [13–15].

Current clarification on the influence mechanism and effect of small atoms in a single structure has been obtained. Hydrogen can exist in stainless steel in many forms due to its small atomic radius, such as interstitial solid solutions, reversibly trapped at defects or internal interfaces, or chemically bound to impurities [16]. Each of these hydrogen states has different effects on the physical and mechanical properties of stainless steel, and these effects include hydrogen embrittlement [17,18], hydrogen-induced increase in dislocation density [19–21], and hydrogen-induced phase transformations [22–24]. In fact, the interface between austenite and ferrite is also considered as a trap site for hydrogen capture. Turnbull and Hutchings [25] regarded both the phase interface and austenite as traps for hydrogen capture, and suggested that the trap effect of austenite was smaller than that of the austenite–ferrite interface. They also think that the presence of austenite makes the diffusion path provided by ferrite more tortuous. In contrast, carbon and nitrogen can only obtain low mobility due to their large atomic radii [26]. Meanwhile, the influence mechanism and effect of these elements on steel is different. Similar to hydrogen, nitrogen can be present in steel by solid solution. It has a positive effect on the formation and stability of austenite, and its effectiveness is about 20 times stronger than that of nickel. Therefore, it can replace some of the nickel in steel within a certain limit [27,28]. However, its introduction may also greatly reduce the ductility and toughness of steel because Fe_4N will be formed [29–31]. The mechanical properties of steel such as strength increase along with the carbon content [32–34], but other properties such as corrosion resistance will be followed by a decrease [35] because the carbon and chromium can form a series of complex compounds [36–39]. For example, the higher the carbon content, the more chromium carbide is formed. At the same time, the corrosion resistance decreases with the decrease in chromium content [40].

Nowadays, the research on interfaces such as grain boundaries [41,42] has been widely reported and made many encouraging achievements. For example, the microscopic mechanisms of the P-induced embrittlement and de-embrittling effect of B and C in ferritic steels were revealed using first principles [43]. This research provides a solid foundation for the development and application of stainless steel. Based on these, the research of the interface and welding [44] of stainless steel has also been greatly developed such as segregation [43], diffusion [45], and repair [46,47]. In these processes, the homojunction provides an effective way to extend the properties of stainless steel. Unfortunately, studies of the intrinsic mechanisms of atomic action at homojunction interfaces are lacking, although relevant experiments have been carried out [48,49].

In this work, the effect of hydrogen, carbon, and nitrogen atoms at the interface on the austenite/ferrite homojunction was investigated using first principles. The homojunction model was composed of α-Fe and γ-Fe. The hydrogen, nitrogen, and carbon atoms were placed at the center of the heterojunction in this study. The effect of a single atom on the heterojunction was studied first. Then, the effect of two identical hydrogen/nitrogen atoms on the heterojunction was studied. The influence of these atoms was analyzed by the energy, density of states (DOS), and electron localization function (ELF). A blank control group was established for comparison with the original homojunction without

small atoms. This study provides valid data and a unique perspective on the development of an austenite/ferrite homojunction.

2. Calculation Details

This work is based on the density functional theory (DFT) in the Vienna Ab-initio Simulation Package (VASP) [50]. The homojunction with 204 atoms is formed by the combination of a 6-layer face-centered-cubic (FCC) structure and a 6-layer body-centered-cubic (BCC) structure. The lengths of the a-axis and b-axis of the FCC and BCC forming the homojunction are 11.3298 Å and 10.9075 Å, respectively, which means that the lattice mismatch (~3.7%) is less than 5%. A vacuum layer of 15 Å is introduced in the c-axis direction to eliminate periodic effects. The atoms are placed at the center of the homojunction. When studying the effect of two atoms on a heterojunction, the initial positions of these atoms are within the van der Waals radius. Binding energy (E_{bind}) is used to characterize the bond between austenite and ferrite. Cohesive energy (E_{coh}) [51,52] and formation enthalpy (E_{form}) are used to discuss the stability of the system. The calculation formulas of these are as follows:

$$E_{bind} = E_{tot} - E_{austenite} - E_{ferrite} \quad (1)$$

where E_{tot} is the total energy of the model, $E_{austenite}$ is the energy of the austenite part, and $E_{ferrite}$ is the energy of the ferrite part.

$$E_{coh} = \frac{1}{n}\left(E_{tot} - \sum x_A E^A_{atom}\right) \quad (2)$$

where n is the total number of atoms, E_{tot} is the total energy of the model, x_A is the number of atoms of type A, and E^A_{atom} is the energy of an isolated type A atom.

$$E_{form} = \frac{1}{n}\left(E_{tot} - \sum x_A E^A_{solid}\right) \quad (3)$$

where n is the total number of atoms, E_{tot} is the total energy of the model, x_A is the number of atoms of type A, and E^A_{solid} is the average energy per atom when A is solid. The energy of hydrogen and nitrogen is replaced by one-half the energy of H_2 and N_2 because they do not exist as a simple solid under normal conditions.

The Perdew–Burke–Ernzerhof (PBE) [53] exchange-correlation functional and Projector Augmented-Wave (PAW) [54,55] pseudopotential are used in this work. We use a cut-off energy of 500 eV to compute all models. The self-consistent field (SCF) convergence threshold is set to 1×10^{-5} eV/atom. All models are optimized for atomic positions, and the force on each ion is less than 0.02 eV/Å. Spin polarization is also considered. A $1 \times 1 \times 1$ k-point grid in the Brillouin region is used in all models. VASPKIT [56] is used in the analysis of DOS. Visualization for Electronic and Structural Analysis (VESTA) [57] is used to draw the model diagram and ELF [58].

3. Results and Discussion

3.1. One Atom at the Interface

First, the pure homojunction was calculated. Its model, ELF, and DOS after optimization are shown in Figure 1.

Metallurgical junctions are formed by distortion of atoms in the two layers near the interface when the FCC and BCC lattices are bonded together. This bonding makes the spin polarization of the atoms at the interface more pronounced. In other words, metallurgical junctions are allowed to form because electrons at the interface change their spin patterns, as shown in Figure 1b. More electrons gather at the interface because the otherwise perfect lattice is distorted to allow pairing with another lattice (see Figure 1c). This charge enrichment is the reason why the interface has strong binding energy (~−29.4801 eV). Anisotropy is introduced into the system [59] because of this combination, which makes stainless steel have high mechanical strength and excellent corrosion resistance [60]. However, lattice dis-

tortion changes the gap at the junction, resulting in a greatly increased probability of atoms with smaller radius entering. This junction becomes a significant weakness in the material despite the strong bond between the two phases. Therefore, hydrogen embrittlement may occur in duplex stainless steel regardless of the phase combination [60]. These are closely related to the behavior of atoms at the interface. For example, Chan et al. [61] suggested that the austenite–martensite interface could capture hydrogen more efficiently than the residual austenite because the hydrogen concentration of retained austenite changes slightly with the increase in carbon content. An important fact is that the austenitic–ferrite interface plays a key role in the hydrogen exchange between adjacent sides, although Turk et al. [15] believed that it was uncertain whether the austenite could be treated as a point trap simply.

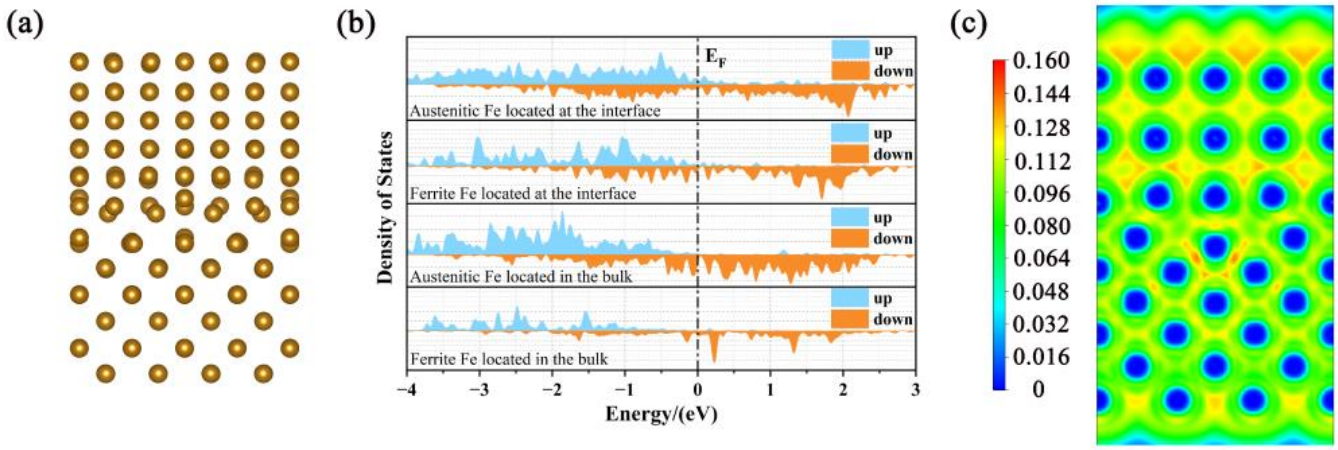


Figure 1. Model, ELF, and DOS of pure homojunction after optimization. (**a**–**c**) The model, DOS, and ELF, respectively. In (**b**), from top to bottom, the DOS of austenitic Fe at the interface, ferrite Fe at the interface, bulk-phase austenitic Fe, and bulk-phase ferrite Fe.

Then, the effect of single atoms on the interface was studied. The model diagram before and after optimization is shown in Figure 2.

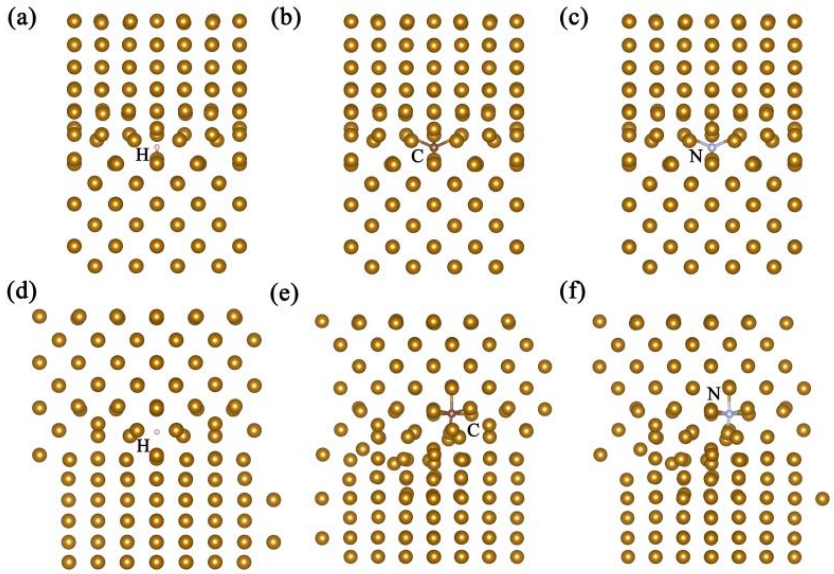


Figure 2. Model diagram before and after optimization. (**a**–**c**) The view of the presence of a H/C/N atom at the interface before optimization, respectively. (**d**–**f**) The view of the presence of a H/C/N atom at the interface after optimization, respectively.

Hydrogen atoms are able to exist at the interfaces because of their smaller atomic radii, while carbon and nitrogen prefer to enter the austenite, as shown in Figure 2. This is consistent with the phenomenon observed in the experiments [16,27–30,62]. A hydrogen atom can interact with multiple iron atoms at the interface and exist in the gap because its radius is very small and there is only one electron in its 1s orbital. In fact, this phase interface acts as not only trap sites for hydrogen capture [10], but also a significant barrier to hydrogen exchange between austenite and ferrite [63] due to the trapping effect. The binding energy of up to 40–50 kJ/mol [10,64,65] at the austenitic–ferrite interface makes it difficult for hydrogen to be released from the trap. The source of this strong binding energy is the significant Coulomb force. The half-full state of the 1s orbital causes electrons moving freely in the crystal field to be attracted to the positively charged hydrogen nuclei. Therefore, hydrogen is difficult to escape from the trap. This trap effect also leads to the diffusion energy barrier of hydrogen jumping from the interface position to the austenite lattice position near the interface as high as 96.7–102.4 kJ/mol [10]. As a result, a large amount of hydrogen is gathered in the interface, which is one of the reasons for fracture. This is not the case for carbon and nitrogen. The octahedral gaps in the FCC lattice can be occupied by carbon/nitrogen atoms, resulting in large lattice distortion energy [62]. This phenomenon is obvious because they need higher energy to cross the interface than hydrogen. At the same time, nitrogen is an austenitic stable element, which makes it remain in the FCC structure. This helps to improve the strength and corrosion resistance [66].

The binding energy, cohesion energy, and enthalpy of formation are shown in Table 1. The DOS and ELF with the presence of a H/C/N atom at the interface was calculated (see Figures 3 and 4).

Table 1. Binding energy, cohesion energy, and enthalpy of formation for the single-atom model.

	E_{bind}/(eV)	E_{coh}/(eV/Atom)	E_{form}/(eV/Atom)
Pure homojunction	−29.4801	−4.5601	0.3003
Homojunction with H	−29.2527	−4.5486	0.2991
Homojunction with C	−32.3280	−4.5686	0.3057
Homojunction with N	−32.4214	−4.5585	0.2782

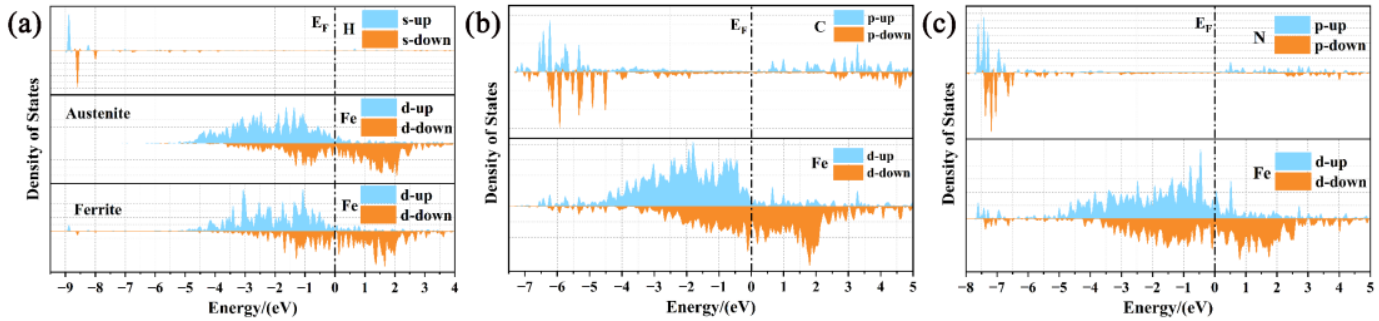


Figure 3. DOS of a H/C/N atom at the interface after optimization. (**a**–**c**) DOS of a H/C/N atom at the interface, respectively.

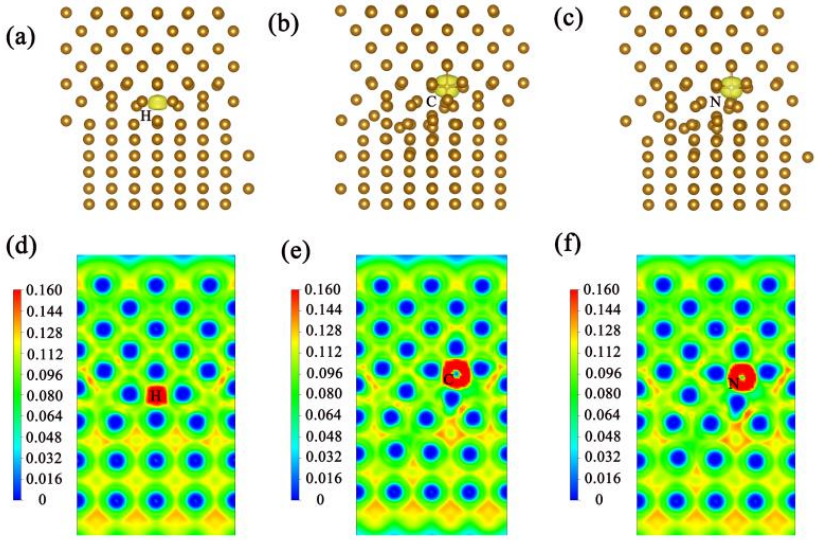


Figure 4. ELF of a H/C/N atom at the interface after optimization. (**a**–**c**) Three-dimensional view of ELF of a H/C/N atom at the interface, respectively. (**d**–**f**) Two-dimensional section view of ELF of a H/C/N atom at the interface, respectively.

Carbon, hydrogen, and nitrogen at the interstitial spaces all lead to charge enrichment, but the effects they cause are different. In the case of hydrogen, it can interact with multiple iron atoms and bind the originally free moving electrons in the lattice because of the special unsaturated valence electron layer. When it is at the interface, the electrons used to form the metallurgical junction are bound by it, which causes the bonding of the interface to be weakened. As a result, the stability of the system is reduced and the interfacial bonding is diminished (see Table 1 and Figures 2 and 3). As mentioned earlier, this phase interface is not only a trap position for hydrogen capture [10], but also an important barrier for hydrogen exchange between austenite and ferrite [63]. Therefore, hydrogen can only enter the interface or remain in the original phase structure and cannot enter other phases through diffusion. Many previous works [17–24] have proved that a large amount of hydrogen is harmful to austenite or ferrite. On the other hand, the electrons used to form the metallurgical junction are attracted by these atoms when they enter the interface, which will greatly weaken the binding force of the metallurgical junction. The opposite result is caused by carbon and nitrogen. They both choose to enter the austenite as interstitial atoms [62]. This not only does not adversely affect interface bonding, but also makes it easier for FCC to pair with BCC due to the local distortion they cause. In fact, the reinforcement of carbon and nitrogen in single-phase structures has been verified by a large number of experiments [66–69]. For duplex stainless steel, Westin [70] reported that nitrogen can be used to reduce chromium-rich nitride such as Cr_2N caused by high ferrite content because it can increase austenite content. This is beneficial to the stability of the interface. The mechanism of this work is similar to it. In theory, the diffusion coefficient of nitrogen in ferrite is two orders of magnitude larger than that in austenite [71]. This is because the diffusion of atoms is directly affected by two factors, namely solubility and diffusivity. The solubility is related to the number of atoms that can remain in the crystal cell. In this case, the austenitic structure can accommodate more nitrogen atoms than the ferrite structure. The diffusivity is related to the ability of atoms to move in the lattice. Therefore, the interstitial atoms can move faster in the BCC structure because the atomic filling factor is lower. For this reason, nitrogen atoms usually diffuse from BCC to FCC. This is also one reason why nitrogen is selected to enter the FCC structure. These nitrogen atoms are used to stabilize FCC to better combine with BCC and facilitate the formation of an interface.

3.2. Two Atoms at the Interface

To further investigate the effect of hydrogen and nitrogen on the austenite/ferrite homojunction, the effect of two hydrogen/nitrogen atoms on the interface was also studied. The model diagram before and after optimization is shown in Figure 5.

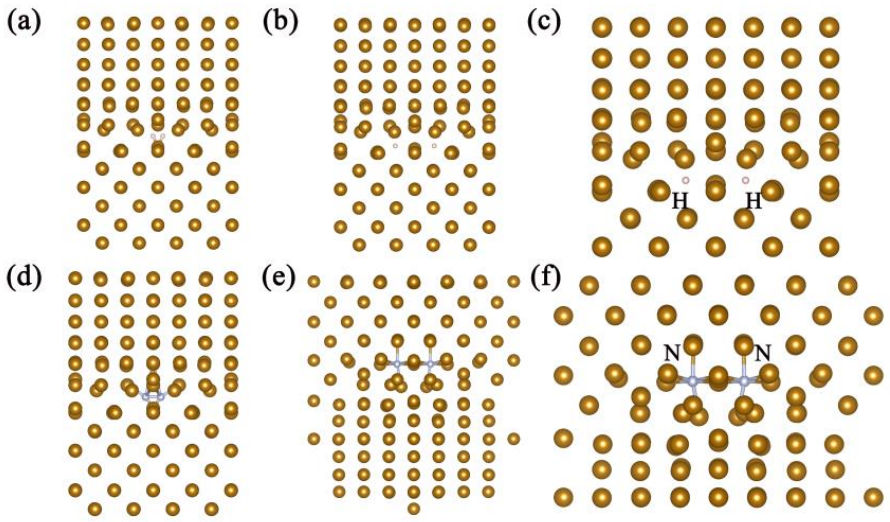


Figure 5. Model diagram before and after optimization. (**a**–**c**) The main view of the presence of two hydrogen atoms at the interface before optimization, and the main view and local enlargement after optimization, respectively. (**d**–**f**) The main view of the presence of two nitrogen atoms at the interface before optimization, and the main view and local enlargement after optimization, respectively.

The atoms will move away from each other and enter adjacent gap sites instead of joining together (see Figure 5). Similar to the case of one hydrogen atom, two hydrogen atoms will move away from each other and enter the adjacent gap, while the nitrogen atoms will enter the two octahedral gaps in the austenite after optimization. This is because the hydrogen atom has a small radius and only one electron [26], which allows it to stay in the interstices of the interface and interact with multiple iron atoms. This is also a result of the capture effect. The 1s half-full state causes electrons moving freely in the crystal field to be attracted to the positively charged hydrogen nuclei. As a result, it is difficult for hydrogen to escape from the trap. Hydrogen atoms are not attracted to each other, because of the enormous coulomb forces, which allows these hydrogen atoms to be dispersed at various places of the interface. On the other hand, the radius of a nitrogen atom is larger than that of hydrogen and its valence electron layer is half full, so it tends to enter austenite, which has been confirmed by numerous studies [62,67,68].

Then, the binding energy, cohesion energy, and enthalpy of formation are shown in Table 2. The DOS and ELF with the presence of two hydrogen/nitrogen atoms at the interface were calculated (see Figures 6 and 7).

Table 2. Binding energy, cohesion energy, and enthalpy of formation for the two-atom model.

	E_{bind}/(eV)	E_{coh}/(eV/Atom)	E_{form}/(eV/Atom)
Homojunction with H	−29.1385	−4.5396	0.2957
Homojunction with N	−29.0240	−4.5912	0.2220

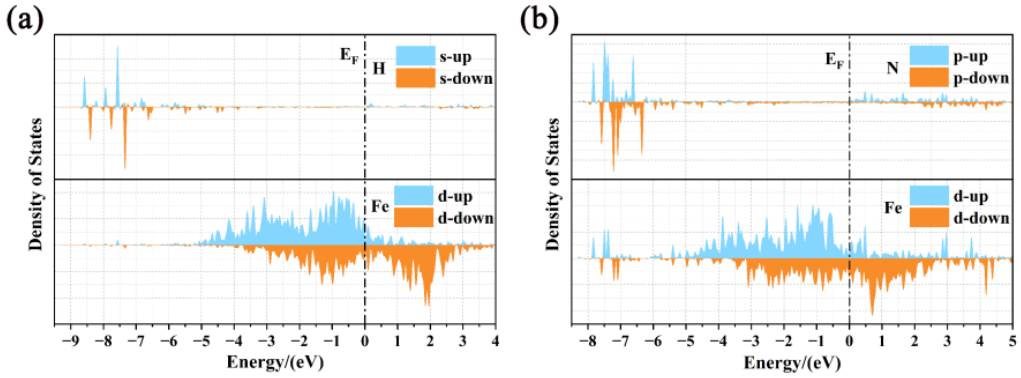


Figure 6. DOS of two atoms at the interface after optimization. (**a**,**b**) The DOS of hydrogen and nitrogen atom at the interface, respectively.

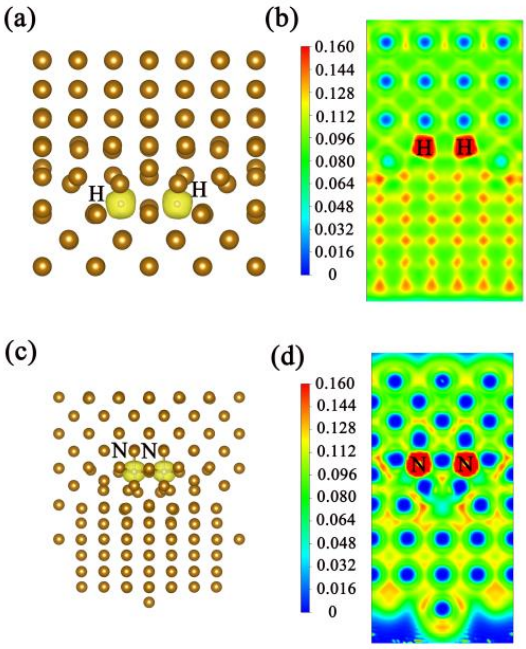


Figure 7. ELF of two atoms at the interface after optimization. (**a**,**b**) Three- and two-dimensional section view of ELF of two hydrogen atoms at the interface, respectively. (**c**,**d**) Three- and two-dimensional section view of ELF of two nitrogen atoms at the interface, respectively.

The effect of hydrogen and nitrogen on homogeneous junctions is very different from the case of Section 3.1 when their concentration increases. The introduction of hydrogen and nitrogen both enriches the charge around them and, thus, weakens the binding of the interface (see Figure 7), but the mechanisms and effects are different. In the case of hydrogen, the small atomic radius and the special structure of only one electron in the 1s orbital allow it to interact with multiple iron atoms at the interface. This allows the interface to combine through hydrogen as a medium, although some electrons are attracted to the bare hydrogen core and, thus, the mobility of hydrogen is affected. Therefore, the binding energy of the hydrogen-containing system is somewhat greater compared to the nitrogen-containing case (see Table 2). E_{coh} and E_{form} also confirm the point that hydrogen-containing systems are more stable than nitrogen-containing systems. This is not inconsistent with the conclusions of previous studies. As described in Section 3.1, the phase interface is not only a trap position for hydrogen capture [10], but also an important barrier for hydrogen exchange between the phases [63]. The hydrogen atoms at the interface can interact with electrons from both the austenite and ferrite parts. In other words, the hydrogen atom can act as a medium, which binds the two phases together by attracting electrons from the two phases.

Therefore, the decrease in binding energy is not as large as that of the system containing hydrogen. This also means that a small amount of hydrogen atoms at the interface may have little effect on the mechanical properties of the interface. However, the intermediation and harmful effects of hydrogen atoms are competitive with each other. The harmful effect caused by a large number of hydrogen atoms at the interface is far greater than the mediating effect they can provide. Therefore, the mechanical properties of the interface will still be seriously reduced if excessive hydrogen atoms are gathered together.

In contrast, nitrogen chooses to become an interstitial atom in the austenite. Its presence enhances the stability of austenite [27,28], but the excessively stable austenite structure at the interface destroys the homogenous state. This is the opposite of low concentration. At low concentrations, hydrogen prevents the migration of electrons at the interface, which reduces the binding energy of the interface and system stability, as shown in Section 3.1. Nitrogen enhances the stability of austenite and allows FCC deformation near the interface to better match with BCC. The result is that the interface binding energy increases and has little impact on the stability of the whole system, as shown in Tables 1 and 2. However, hydrogen can act as a mediator between the two phases at the interface when the concentration increases. In contrast, nitrogen that can only enter the austenite will overstrengthen the FCC phase. In this case, it is difficult for the FCC structure near the interface to distort and match with BCC. This, in turn, destroys the balance of the interface, resulting in a rapid decline in the stability of the system. Therefore, the binding energy is lower than that of hydrogen (see Table 2). One of the conditions for the formation of an interface is that several atomic layers on either side of the interface are allowed to distort and pair with each other. However, the enrichment of nitrogen atoms will make it difficult for these atomic layers to distort and pair with each other. Therefore, the interface formed in this case is unstable. An unstable interface is a weakness for mechanical properties. Similar to the second-phase strengthening mechanism, it will also lead to the potential initiation of cracks near the interface, which plays a positive role in the fracture of materials.

4. Conclusions

In this study, the effects of hydrogen, carbon, and nitrogen atoms at the interface on the austenite/ferrite homojunction were investigated using first principles. The conclusions are summarized as follows:

(1) Carbon and nitrogen can effectively strengthen austenite at low concentration, and the local distortion produced in the process is conducive to the combination and stable existence of the interface.
(2) At low concentration, the bonding energy and stability of the C/N-containing system are better than those of the hydrogen-containing system.
(3) A high concentration of hydrogen and nitrogen will reduce the binding energy of the interface. However, the hydrogen can partially act as the interfacial binding medium, which makes the binding energy decrease more slowly.
(4) The high concentration of nitrogen causes the austenite to over-strengthen, which leads to a sharp decline in interface matching. Therefore, the binding energy of the interface and the stability of the whole system are reduced.

This study provides valid data and a unique perspective on the development of an austenite/ferrite homojunction.

Author Contributions: Conceptualization, X.Z. (Xinghua Zhu) and Y.X.; software, Q.F.; data curation, X.Z. (Xinghua Zhu), B.C. and L.X.; funding acquisition, Y.X., X.Z. (Xiaoyang Zhu) and Z.H.; investigation, X.Z. (Xinghua Zhu), B.C. and J.H.; resources, Q.F.; writing—original draft preparation, X.Z. (Xinghua Zhu); writing—review and editing, Y.X.; supervision, Y.X.; visualization, Y.X. and Z.H. All authors have read and agreed to the published version of the manuscript.

Funding: This work was supported by the Science and Technology on Reactor Fuel and Materials Laboratory, Key R&D projects in the field of high and new Technology of Sichuan Province (20ZDYF0490, 20ZDYF0236), and the National Key Project of Research and Development Program of China (2016YFB1100202). The authors thank the Sichuan Liuhe Special Metal Materials Co. LTD for financial support.

Institutional Review Board Statement: Not applicable.

Informed Consent Statement: Not applicable.

Data Availability Statement: The data presented in this study are available on request from the corresponding author.

Acknowledgments: The authors are grateful to Zhou Liu for the helpful discussion and constructive comments on the manuscript.

Conflicts of Interest: The authors declare no conflict of interest.

References

1. Was, G.S.; Ukai, S. Chapter 8-Austenitic Stainless Steels. In *Structural Alloys for Nuclear Energy Applications*; Odette, G.R., Zinkle, S.J., Eds.; Elsevier: Boston, MA, USA, 2019; pp. 293–347. [CrossRef]
2. Lo, K.H.; Shek, C.H.; Lai, J.K.L. Recent developments in stainless steels. *Mater. Sci. Eng. R Rep.* **2009**, *65*, 39–104. [CrossRef]
3. Lula, R.A. *Stainless Steel*; American Society for Metals: Metals Park, OH, USA, 1985.
4. Beddoes, J.; Parr, J. *Introduction to Stainless Steels*, 3rd ed.; ASM International: Materials Park, OH, USA, 1999.
5. Şahin, S.; Übeyli, M. A Review on the Potential Use of Austenitic Stainless Steels in Nuclear Fusion Reactors. *J. Fusion Energy* **2008**, *27*, 271–277. [CrossRef]
6. Avner, S.H. *Introduction to Physical Metallurgy*; McGraw-Hill, Inc: 1325 Avenue of the Americas, New York, NY, USA, 1964.
7. Handbook of Stainless Steels. *Br. Corros. J.* **1978**, *13*, 56. [CrossRef]
8. Ooi, S.W.; Hill, P.; Rawson, M.; Bhadeshia, H.K.D.H. Effect of retained austenite and high temperature Laves phase on the work hardening of an experimental maraging steel. *Mater. Sci. Eng. A* **2013**, *564*, 485–492. [CrossRef]
9. Viswanathan, U.K.; Dey, G.K.; Asundi, M.K. Precipitation Hardening in 350 Grade Maraging Steel. *MMTA* **1993**, *24*, 2429–2442. [CrossRef]
10. Wu, W.; Zhang, X.; Li, W.; Fu, H.; Liu, S.; Wang, Y.; Li, J. Effect of hydrogen trapping on hydrogen permeation in a 2205 duplex stainless steel: Role of austenite–ferrite interface. *Corros. Sci.* **2022**, *202*, 110332. [CrossRef]
11. Olden, V.; Thaulow, C.; Johnsen, R. Modelling of hydrogen diffusion and hydrogen induced cracking in supermartensitic and duplex stainless steels. *Mater. Des.* **2008**, *29*, 1934–1948. [CrossRef]
12. Jackson, H.F.; Nibur, K.A.; San Marchi, C.; Puskar, J.D.; Somerday, B.P. Hydrogen-assisted crack propagation in 304L/308L and 21Cr–6Ni–9Mn/308L austenitic stainless steel fusion welds. *Corros. Sci.* **2012**, *60*, 136–144. [CrossRef]
13. Owczarek, E.; Zakroczymski, T. Hydrogen transport in a duplex stainless steel. *Acta Mater.* **2000**, *48*, 3059–3070. [CrossRef]
14. Zakroczymski, T.; Owczarek, E. Electrochemical investigation of hydrogen absorption in a duplex stainless steel. *Acta Mater.* **2002**, *50*, 2701–2713. [CrossRef]
15. Turk, A.; Pu, S.D.; Bombač, D.; Rivera-Díaz-del-Castillo, P.E.J.; Galindo-Nava, E.I. Quantification of hydrogen trapping in multiphase steels: Part II – Effect of austenite morphology. *Acta Mater.* **2020**, *197*, 253–268. [CrossRef]
16. Borchers, C.; Michler, T.; Pundt, A. Effect of Hydrogen on the Mechanical Properties of Stainless Steels. *Adv. Eng. Mater.* **2008**, *10*, 11–23. [CrossRef]
17. Whiteman, M.B.; Troiano, A.R. Hydrogen Embrittlement Of Austenitic Stainless Steel. *Corrosion* **2013**, *21*, 53–56. [CrossRef]
18. Murakami, Y.; Kanezaki, T.; Mine, Y.; Matsuoka, S. Hydrogen Embrittlement Mechanism in Fatigue of Austenitic Stainless Steels. *MMTA* **2008**, *39*, 1327–1339. [CrossRef]
19. Gavriljuk, V.G.; Shivanyuk, V.N.; Foct, J. Diagnostic experimental results on the hydrogen embrittlement of austenitic steels. *Acta Mater.* **2003**, *51*, 1293–1305. [CrossRef]
20. Ferreira, P.J.; Robertson, I.M.; Birnbaum, H.K. Hydrogen effects on the interaction between dislocations. *Acta Mater.* **1998**, *46*, 1749–1757. [CrossRef]
21. Barnoush, A.; Vehoff, H. Electrochemical nanoindentation: A new approach to probe hydrogen/deformation interaction. *Scr. Mater.* **2006**, *55*, 195–198. [CrossRef]
22. Bugaev, V.N.; Gavriljuk, V.G.; Petrov, Y.N.; Tarasenko, A.V. Mechanism of hydrogen-induced phase transformations in metals and alloys. *Int. J. Hydrogen Energy* **1997**, *22*, 213–218. [CrossRef]
23. Vakhney, A.G.; Yaresko, A.N.; Antonov, V.N.; Nemoshkalenko, V.V. The effect of hydrogen on the electronic structure and cohesive properties of iron-based alloys doped by chromium and nickel. *Int. J. Hydrogen Energy* **2001**, *26*, 453–456. [CrossRef]
24. Tsay, L.W.; Yu, S.C.; Huang, R.T. Effect of austenite instability on the hydrogen-enhanced crack growth of austenitic stainless steels. *Corros. Sci.* **2007**, *49*, 2973–2984. [CrossRef]

25. Turnbull, A.; Hutchings, R.B. Analysis of hydrogen atom transport in a two-phase alloy. *Mater. Sci. Eng. A* **1994**, *177*, 161–171. [CrossRef]
26. Haynes, W. *CRC Handbook of Chemistry and Physics*; CRC: Boca Raton, FL, USA, 2012; Volume 94.
27. Byrnes, M.L.G.; Grujicic, M.; Owen, W.S. Nitrogen strengthening of a stable austenitic stainless steel. *Acta Metall.* **1987**, *35*, 1853–1862. [CrossRef]
28. Reed, R.P. Nitrogen in austenitic stainless steels. *JOM* **1989**, *41*, 16–21. [CrossRef]
29. Mingolo, N.; Tschiptschin, A.P.; Pinedo, C.E. On the formation of expanded austenite during plasma nitriding of an AISI 316L austenitic stainless steel. *Surf. Coat. Technol.* **2006**, *201*, 4215–4218. [CrossRef]
30. Xu, X.; Wang, L.; Yu, Z.; Qiang, J.; Hei, Z. Study of microstructure of low-temperature plasma-nitrided AISI 304 stainless steel. *MMTA* **2000**, *31*, 1193–1199. [CrossRef]
31. Martinavičius, A.; Abrasonis, G.; Scheinost, A.C.; Danoix, R.; Danoix, F.; Stinville, J.C.; Talut, G.; Templier, C.; Liedke, O.; Gemming, S.; et al. Nitrogen interstitial diffusion induced decomposition in AISI 304L austenitic stainless steel. *Acta Mater.* **2012**, *60*, 4065–4076. [CrossRef]
32. Michal, G.M.; Ernst, F.; Heuer, A.H. Carbon paraequilibrium in austenitic stainless steel. *MMTA* **2006**, *37*, 1819–1824. [CrossRef]
33. Cao, Y.; Ernst, F.; Michal, G.M. Colossal carbon supersaturation in austenitic stainless steels carburized at low temperature. *Acta Mater.* **2003**, *51*, 4171–4181. [CrossRef]
34. Sun, Y.; Li, X.; Bell, T. Low temperature plasma carburising of austenitic stainless steels for improved wear and corrosion resistance. *Surf. Eng.* **1999**, *15*, 49–54. [CrossRef]
35. Vitos, L.; Korzhavyi, P.A.; Johansson, B. Elastic Property Maps of Austenitic Stainless Steels. *Phys. Rev. Lett.* **2002**, *88*, 155501. [CrossRef]
36. Ha, H.-Y.; Lee, T.-H.; Oh, C.-S.; Kim, S.-J. Effects of Carbon on the Corrosion Behaviour in Fe-18Cr-10Mn-N-C Stainless Steels. *Steel Res. Int.* **2009**, *80*, 488–492.
37. Sun, Y. Depth-profiling electrochemical measurements of low temperature plasma carburised 316L stainless steel in 1M H2SO4 solution. *Surf. Coat. Technol.* **2010**, *204*, 2789–2796. [CrossRef]
38. Niu, W.; Lillard, R.S.; Li, Z.; Ernst, F. Properties of the Passive Film Formed on Interstitially Hardened AISI 316L Stainless Steel. *Electrochim. Acta* **2015**, *176*, 410–419. [CrossRef]
39. Niu, W.; Li, Z.; Ernst, F.; Lillard, R.S. The passivity of low-temperature carburized austenitic stainless steel AISI-316L in a simulated boiling-water-reactor environment. *J. Nucl. Mater.* **2020**, *537*, 152197. [CrossRef]
40. Tedmon, C.S.; Vermilyea, D.A.; Rosolowski, J.H. Intergranular Corrosion of Austenitic Stainless Steel. *J. Electrochem. Soc.* **1971**, *118*, 192. [CrossRef]
41. Mengzhe, H.; Weigang, C.; Ying, X.; Fucheng, Z.; Bo, L. First-principles study of the effect of N on the ∑5 (210) [001] grain boundary of γ-Fe. *Mater. Today Commun.* **2022**, *33*, 104496. [CrossRef]
42. Liu, T.; Hui, J.; Zhang, B.; He, X.; Liu, M.; Qiu, J.; Liu, W. Corrosion mechanism of lead-bismuth eutectic at grain boundary in ferritic steels and the effect of alloying elements: A first-principles study. *J. Nucl. Mater.* **2022**, *569*, 153915. [CrossRef]
43. Wang, J.; Enomoto, M.; Shang, C. First-principles study on the P-induced embrittlement and de-embrittling effect of B and C in ferritic steels. *Acta Mater.* **2021**, *219*, 117260. [CrossRef]
44. Suutala, N.; Takalo, T.; Moisio, T. Ferritic-austenitic solidification mode in austenitic stainless steel welds. *Metall. Trans. A* **1980**, *11*, 717–725. [CrossRef]
45. Agarwala, R.P.; Naik, M.C.; Anand, M.S.; Paul, A.R. Diffusion of carbon in stainless steels. *J. Nucl. Mater.* **1970**, *36*, 41–47. [CrossRef]
46. Graf, B.; Gumenyuk, A.; Rethmeier, M. Laser Metal Deposition as Repair Technology for Stainless Steel and Titanium Alloys. *Phys. Procedia* **2012**, *39*, 376–381. [CrossRef]
47. AghaAli, I.; Farzam, M.; Golozar, M.A.; Danaee, I. The effect of repeated repair welding on mechanical and corrosion properties of stainless steel 316L. *Mater. Des. (1980-2015)* **2014**, *54*, 331–341. [CrossRef]
48. Mo, D.-f.; Song, T.-f.; Fang, Y.-j.; Jiang, X.-s.; Luo, C.Q.; Simpson, M.D.; Luo, Z.-p. A Review on Diffusion Bonding between Titanium Alloys and Stainless Steels. *Adv. Mater. Sci. Eng.* **2018**, *2018*, 8701890. [CrossRef]
49. Orhan, N.; Khan, T.I.; Eroğlu, M. Diffusion bonding of a microduplex stainless steel to Ti–6Al–4V. *Scr. Mater.* **2001**, *45*, 441–446. [CrossRef]
50. Kresse, G.; Furthmüller, J. Efficiency of ab-initio total energy calculations for metals and semiconductors using a plane-wave basis set. *Comput. Mater. Sci.* **1996**, *6*, 15–50. [CrossRef]
51. Ding, Y.; Wang, Y. Unusual structural and electronic properties of porous silicene and germanene: Insights from first-principles calculations. *Nanoscale Res. Lett.* **2015**, *10*, 13. [CrossRef]
52. Bai, H.; Zhu, Y.; Qiao, W.; Huang, Y. Structures, stabilities and electronic properties of graphdiyne nanoribbons. *RSC Adv.* **2011**, *1*, 768–775. [CrossRef]
53. Perdew, J.P.; Burke, K.; Ernzerhof, M. Generalized Gradient Approximation Made Simple. *Phys. Rev. Lett.* **1996**, *77*, 3865–3868. [CrossRef]
54. Blöchl, P.E. Projector augmented-wave method. *PhRvB* **1994**, *50*, 17953–17979. [CrossRef]
55. Kresse, G.; Joubert, D. From ultrasoft pseudopotentials to the projector augmented-wave method. *PhRvB* **1999**, *59*, 1758–1775. [CrossRef]

56. Wang, V.; Xu, N.; Liu, J.-C.; Tang, G.; Geng, W.-T. VASPKIT: A user-friendly interface facilitating high-throughput computing and analysis using VASP code. *Comput. Phys. Commun.* **2021**, *267*, 108033. [CrossRef]
57. Momma, K.; Izumi, F. VESTA 3 for three-dimensional visualization of crystal, volumetric and morphology data. *J. Appl. Crystallogr.* **2011**, *44*, 1272–1276. [CrossRef]
58. Becke, A.D.; Edgecombe, K.E. A simple measure of electron localization in atomic and molecular systems. *J. Chem. Phys.* **1990**, *92*, 5397–5403. [CrossRef]
59. Young, M.C.; Chan, S.L.I.; Tsay, L.W.; Shin, C.S. Hydrogen-enhanced cracking of 2205 duplex stainless steel welds. *Mater. Chem. Phys.* **2005**, *91*, 21–27. [CrossRef]
60. da Silva, B.R.S.; Salvio, F.; Santos, D.S.d. Hydrogen induced stress cracking in UNS S32750 super duplex stainless steel tube weld joint. *Int. J. Hydrogen Energy* **2015**, *40*, 17091–17101. [CrossRef]
61. Chan, S.L.I.; Lee, H.L.; Yang, J.R. Effect of retained austenite on the hydrogen content and effective diffusivity of martensitic structure. *Metall. Trans. A* **1991**, *22*, 2579–2586. [CrossRef]
62. Oda, K.; Kondo, N.; Shibata, K. X-ray Absorption Fine Structure Analysis of Interstitial (C, N)-Substitutional (Cr) Complexes in Austenitic Stainless Steels. *ISIJ Int.* **1990**, *30*, 625–631. [CrossRef]
63. Mente, T.; Bollinghaus, T. Modeling Of Hydrogen Distributionin A Duplex Stainless Steel. *Weld. World* **2012**, *56*, 66–78. [CrossRef]
64. Silverstein, R.; Sobol, O.; Boellinghaus, T.; Unger, W.; Eliezer, D. Hydrogen behavior in SAF 2205 duplex stainless steel. *J. Alloys Compd.* **2017**, *695*, 2689–2695. [CrossRef]
65. Dabah, E.; Lisitsyn, V.; Eliezer, D. Performance of hydrogen trapping and phase transformation in hydrogenated duplex stainless steels. *Mater. Sci. Eng. A* **2010**, *527*, 4851–4857. [CrossRef]
66. Li, T.; Chien, S.-C.; Ren, Z.; Windl, W.; Ernst, F.; Frankel, G.S. Understanding the efficacy of concentrated interstitial carbon in enhancing the pitting corrosion resistance of stainless steel. *Acta Mater.* **2021**, *221*, 117433. [CrossRef]
67. Berns, H.; Gavriljuk, V.; Shanina, B. Intensive Interstitial Strengthening of Stainless Steels. *Adv. Eng. Mater.* **2008**, *10*, 1083–1093. [CrossRef]
68. Shankar, P.; Sundararaman, D.; Ranganathan, S. Clustering and ordering of nitrogen in nuclear grade 316LN austenitic stainless steel. *J. Nucl. Mater.* **1998**, *254*, 1–8. [CrossRef]
69. Ledbetter, H.M.; Austin, M.W. Effects of carbon and nitrogen on the elastic constants of AISI type 304 stainless steel. *MSEng* **1985**, *70*, 143–149. [CrossRef]
70. Westin, E.M. Microstructure and Properties of Welds in the Lean Duplex Stainless Steel LDX 2101. Ph.D. Thesis, Comprehensive Summary. KTH, Stockholm, Sweden, 2010.
71. Bobadilla, M.; Tschiptschin, A. On the Nitrogen Diffusion in a Duplex Stainless Steel. *Mater. Res.* **2015**, *18*, 390–394. [CrossRef]

Disclaimer/Publisher's Note: The statements, opinions and data contained in all publications are solely those of the individual author(s) and contributor(s) and not of MDPI and/or the editor(s). MDPI and/or the editor(s) disclaim responsibility for any injury to people or property resulting from any ideas, methods, instructions or products referred to in the content.